Hydrogen bond directed molecular recognition in water in a strapped-porphyrin-cyclodextrin assembly

Hiroaki Kitagishi*[a], Kazuki Ohara[a], Daiki Shimoji[a], Maxime Vonesch[b], Jean Weiss[b◊] and Jennifer A. Wytko*[b◊]

[a] *Department of Molecular Chemistry and Biochemistry, Faculty of Science and Engineering, Doshisha University, Kyotanabe, Kyoto 610-0321, Japan*
[b] *Institut de Chimie de Strasbourg, UMR 7177, CNRS, Université de Strasbourg, 4 Rue Blaise Pascal, 67000 Strasbourg, France*

This paper is part of the 2019 Women in Porphyrin Science special issue.

ABSTRACT: A water soluble, phenanthroline-strapped zinc porphyrin bearing four arylsulfonate groups formed a stable host–guest complex with two per-*O*-methylated β-cyclodextrin cavities. In the host–guest assembly, the zinc porphyrin was capable of binding imidazole within the cavity between the zinc(II) ion and the phenanthroline strap in an aqueous medium. The formation of a hydrogen bond between the imidazole NH and the nitrogen atoms of the phenanthroline was an essential element of the binding event, as shown by comparative binding studies with a non-strapped tetrasulfonated zinc porphyrin and with *N*-methylimidazole. This hydrogen bonding in an aqueous medium was possible due to the protected hydrophobic environment created by the cyclodextrins around the phenanthroline strap. This type of binding event may provide a biomimetic approach to study water soluble hemeprotein models.

KEYWORDS: hydrogen bonding, aqueous medium, host–guest complex, β-cyclodextrin, porphyrin.

INTRODUCTION

The development of heme protein models has been a challenge for more than four decades. Prior to the emergence of X-ray diffraction, the initial concern was the identification and characterization of active sites in natural systems. Iron porphyrins or *hemes* were clearly identified as the main component of the active site of a large class of enzymes and proteins, but the efficient synthesis of these active sites was also a challenge at that time. One difficulty lies in differentiating both faces of the porphyrin macrocycle. The proximal face corresponds to the face that bears a ligand in close proximity to the central iron core, whereas on the distal face, the reactivity and accessibility of the heme iron center, is controlled by distant residues.

Utilization of nitro-aryl-aldehydes allowed the preparation of a basic building block, namely the *meso*-tetraaminophenyl porphyrin [1] that could be further functionalized to fine tune the distal site of the heme, hence paving the way to further-refined functions of the models [2]. Surprisingly, the basic design concepts of heme protein models have evolved much less than our understanding of the complexity in controlling heme reactivity in natural systems *via* protein mutations or heme substitution [3], the use of small peptide-appended porphyrins [4] or the noncovalent association of synthetic hemes with monoclonal antibodies [5]. The field of synthetic heme protein models seems to have reached a conceptual steady state in which efficient mimics are too complicated for applications to be developed, and models are too simple and do not perform well enough.

A notable innovation associated simple commercial iron porphyrins with an exogenic environment consisting

◊ SPP full member in good standing

*Correspondence to: H. Kitagishi, tel.: +81-774-65-7442, email: hkitagis@mail.doshisha.ac.jp; J. Wytko, tel.: +33-368-85-14-24, email: jwytko@unistra.fr.
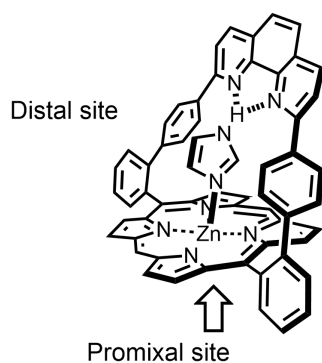
Fig. 1. A phenanthroline-strapped zinc porphyrin with an imidazole bound at the distal site, defined by the phenanthroline pocket. The proximal site is the open face of the zinc porphyrin

in a functionalized β-cyclodextrin (β-CD) host rather than just an exogenic proximal base [6]. CDs are a widely studied class of host molecules possessing an internal hydrophobic cavity and an external hydrophilic envelope. The inclusion of iron porphyrins within cyclodextrins provides water-soluble heme models with a hydrophobic environment above the porphyrin macrocycle [7] and can be complemented by ligand coordination at the proximal site of the metal [8]. A set of significant studies has emerged from this novel approach and the results are extremely encouraging [9, 10]. For example, a myoglobin model capable of oxygen binding in aqueous media was able to deplete endogenous carbon monoxide selectively [11]. However, to date, only commercially available porphyrins have been engaged in these studies.

Our groups have taken advantage of an accessible phenanthroline-strapped porphyrin to develop new bioinorganic models that contain a generic predefined distal binding site as summarized in Fig. 1 [12, 13]. A tremendous advantage of the phenanthroline-strapped structure is its synthetic availability on a gram scale within a few weeks. Over the last decade, the selective

imidazole recognition [14, 15] within the phenanthroline strap was used to construct a family of supramolecular complexes that mimic the hetero-binuclear site of cytochrome *c* oxidase [12, 16]. Very simple derivatives of this strapped porphyrin can be sulfonated (Scheme 1) to favor their inclusion within β-CD hosts. We report herein the formation of a host–guest complex between a synthetic phenanthroline-strapped porphyrin and per-*O*-methylated β-CD and we provide evidence for the selective distal binding of N–H imidazoles induced by hydrogen bonding in aqueous media.

RESULTS AND DISCUSSION

The sulfonated strapped porphyrin was synthesized in three steps starting from the dibromo-porphyrin **1** [15], as shown in Scheme 1. The latter was reacted with phenyl boronic acid under classical biphasic Suzuki cross-coupling conditions to afford the bis(*meso*-phenyl)-strapped porphyrin **2** in 49% yield. Compound **2** was then sulfonated in concentrated sulfuric acid to afford the tetrasulfonated derivative **3** in 65% yield as its ammonium salt. In addition to the high yield, the sulfonation reaction was extremely regioselective. The only isomer that was isolated and characterized by 1D and 2D ^{1}H NMR (^{1}H–^{1}H COSY) experiments is the derivative represented in Scheme 1, with one sulfonate group on each of the four *meso*-phenyl rings. Treatment of **3** with excess ZnO in water led to the metallated porphyrin **3Zn** in 26% yield. In an attempt to improve the yield of this last step, excess Zn(OAc)$_2$ was reacted with **3** in THF/MeOH/pyridine. The use of Zn(OAc)$_2$, which can also act as a Lewis acid, led to the regioselective removal of two of the four sulfonate groups as well as metalation to afford **4Zn** in 62% yield. The limited solubility of **4Zn** in buffered aqueous media prevented further inclusion studies with β-CD.

The interaction of the sulfonated strapped porphyrin with permethylated β-CD (TMe-β-CD) was investigated
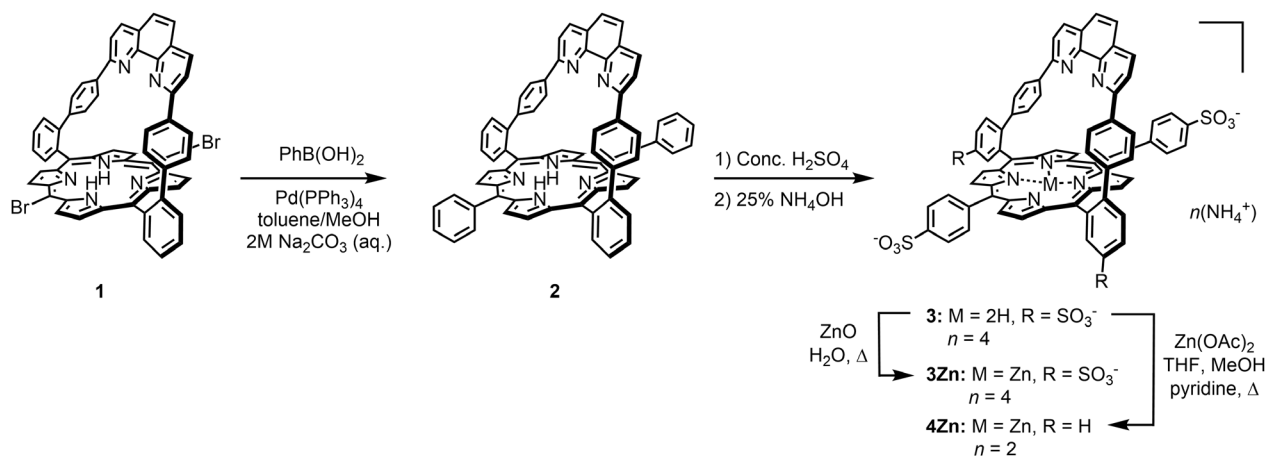
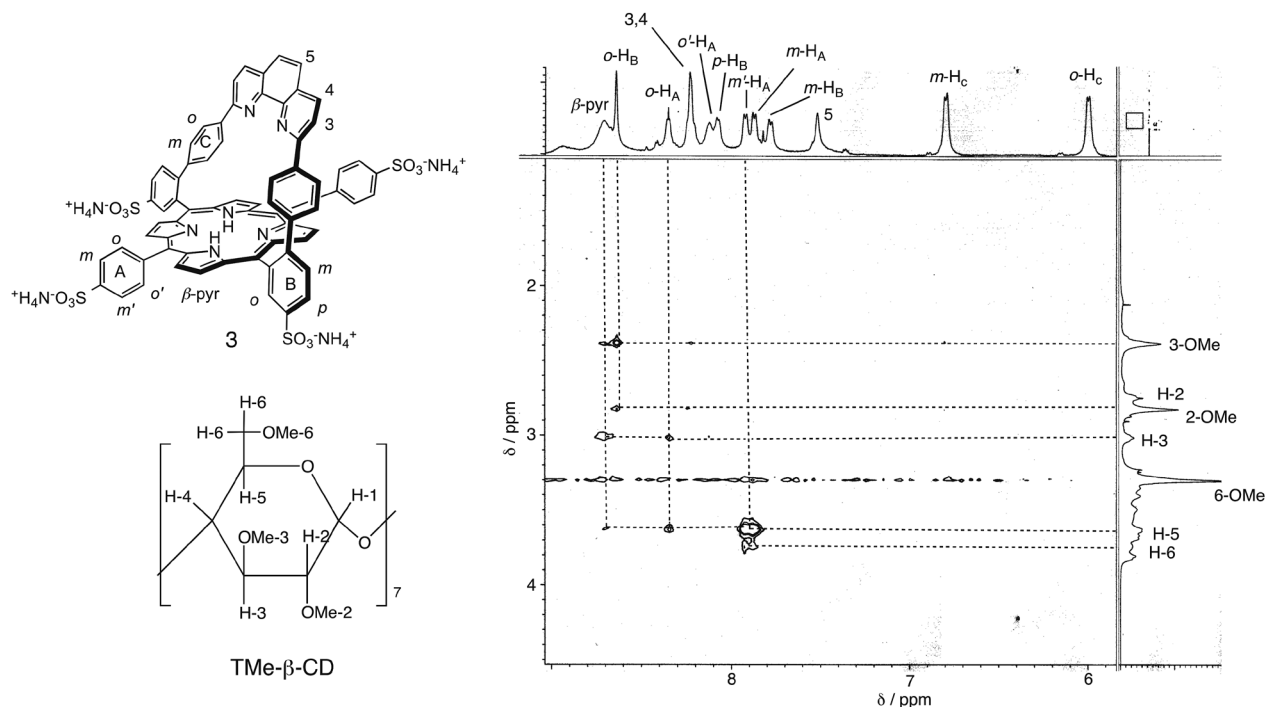**Scheme 1.** Synthesis of sulfonated zinc porphyrins

Fig. 2. ROESY NMR spectrum of the 2:1 TMe-β-CD/**3** complex ([TMe-β-CD] = 2 mM, [**3**] = 1 mM) in D$_2$O at 25 °C. The mixing time was 0.25 s

by UV-vis and ^{1}H NMR spectroscopies for **3** and **3Zn** in aqueous media. Titrations of **3** or **3Zn** yielded a new species which ceased to evolve after the addition of two equivalents of TMe-β-CD, thus confirming the stoichiometry of the supramolecular inclusion complex formed (see SI). In particular, the ROESY spectrum (Fig. 2) of a 2:1 mixture of TMe-β-CD/**3** in D$_2$O shows the close proximity of protons H-5 and H-6 in the cyclodextrin to the m-H$_A$ and m′-H$_A$ protons of the aromatic ring A (indicated in Fig. 2), which is *para*-substituted with a sulfonate group. No correlations were seen between the CD protons and the *para* and *meta* protons p-H$_B$ and m-H$_B$ of aromatic ring B. Together, these observations confirm the inclusion of phenyl rings A within CD cavities. Interactions between the methoxy groups at the 3 position (H-3 and 3-OMe in Fig. 2) of the cyclodextrin and the porphyrin's β-pyrrolic protons (labelled β-pyr) indicate that the secondary face of the cyclodextrin protects two opposite sides of the porphyrin, as previously observed for the inclusion of the non-strapped tetraphenylporphyrin sulfonate (TPPS) within TMe-β-CD [17].

The stability constants (Table 1) for the successive equilibria of **3** and **3Zn** bound in one or two TMe-β-CD cavities were determined by UV-vis titrations in a 0.05 M phosphate buffer (see SI). The binding constants of both **3** and **3Zn** with TMe-β-CD are of the same order of magnitude. These stability constants were smaller than for porphyrin systems without a strap [17]; however, the values suggest that the intermolecular

Table 1. The binding constants (*K*) for the formation of 1:1 and 2:1 complexation of TMe-β-CD with **3** and **3Zn** in 0.05 M phosphate buffer at pH 7 and 25 °C[a]

Compound	K_1 (M^{-1})	K_2 (M^{-1})
3	1.8×10^6	3.5×10^5
3Zn	1.5×10^6	6.7×10^5

[a]The binding constants were determined from UV-vis titration experiments. The titration curves were analyzed using an equation for the 1:1 and 1:2 equilibria.

interactions are still strong and the inclusion occurs quantitatively, even in dilute aqueous media.

Among the peculiar properties of the phenanthroline-strapped Zn porphyrin architectures is their ability to bind imidazoles very selectively in the phenanthroline strap in chlorinated solvents [14, 15] (Fig. 1). In this binding event, the relative inaccessibility of the metal is compensated by the formation of a bifurcated hydrogen bond between the imidazole N–H and the nitrogen atoms of the phenanthroline. This phenomenon is markedly strong in chlorinated solvents. The aim of the present work is to determine if such selectivity could be observed in aqueous media, taking advantage of the protective presence of the cyclodextrins around the
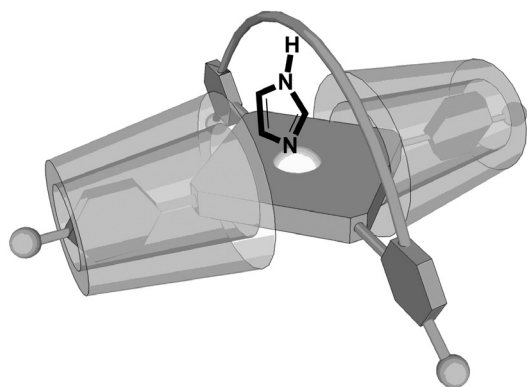
Fig. 3. Schematic representation of the 2:1 TMe-β-CD/**3** complex with an imidazole bound within the phenanthroline strap

Table 2. The binding constants (K) for the coordination of imidazole (ImH) and N-methylimidazole (N-MeIm) to the Zn porphyrin complexes without and with TMe-β-CD in 0.05 M phosphate buffer at pH 7 and 25 °C[a]

Host	K (M^{-1})	
	ImH	N-MeIm
3Zn	17	4
3Zn-(TMe-β-CD)$_2$	195	[b]
ZnTPPS	75	77
ZnTPPS-(TMe-β-CD)$_2$	69	15

[a] The binding constants were determined based on the UV-vis titration experiments. The titration curves were analyzed using an equation for a 1:1 equilibrium. [b] Too small to be determined.

strapped porphyrin in the **3Zn**(TMe-β-CD)$_2$ host–guest complex, as depicted schematically in Fig. 3. Therefore, UV-vis absorption titrations with imidazole (ImH) were performed in aqueous media for the porphyrin-TMe-β-CD supramolecular assemblies **3Zn**-(TMe-β-CD)$_2$. For comparison purposes, similar titrations were performed with **3Zn**, the parent ZnTPPS and ZnTPP-(TMe-β-CD)$_2$. The effects of the hydrogen bonding were evaluated by comparative titrations with N-methylimidazole (N-MeIm), which cannot form a hydrogen bond with the phenanthroline nitrogen atoms. Table 2 summarizes the binding constants determined for the formation of the ternary pentacoordinated zinc complexes.

Binding of ImH in the phenanthroline pocket of **3Zn** was still effective in water, but much more so when protected by the cyclodextrins (see Table 2). In the presence of cyclodextrins, the binding of ImH to **3Zn**-(TMe-β-CD)$_2$ is enhanced ten times relative to with **3Zn** alone. When the hydrogen bonding site is unprotected, the aqueous environment perturbs the

formation of a hydrogen bond between the pyrrolic proton of the ImH and the phenanthroline [17]. In the absence of the protective cyclodextrin environment, **3Zn** displayed a significantly reduced affinity for both ImH and N-MeIm compared to ZnTPPS. This decrease is ascribed to the steric hindrance on one face of **3Zn** which limits the access for ligand-metal binding. In terms of selectivity, the affinity of **3Zn** for ImH is still four times higher than for N-MeIm despite the difference in pK_a values and the higher basicity of N-MeIm. Although ImH and N-MeIm can both bind to the zinc center of **3Zn**, the greater affinity of ImH suggests that, for this substrate, a hydrogen bond still forms with the phenanthroline strap.

In comparison, the affinity of ZnTPPS-(TMe-β-CD)$_2$ for N-MeIm is four times lower than in the absence of TMe-β-CDs, reflecting the increased steric bulk around the zinc dz^2 orbital, which is responsible for the axial base coordination. This steric bulk explains why the equilibrium constant for the formation of a ternary complex between **3Zn**-(TMe-β-CD)$_2$ and N-MeIm was too low to be measured. Based on the above, the distal site selectivity of **3Zn**-(TMe-β-CD)$_2$ and the enhanced binding of ImH vs. N-Im can be attributed to the formation of a hydrogen bond between the ImH and the phenanthroline, in addition to metal-ligand binding. The TMe-β-CDs provide a microscopically apolar environment [18] that protects the hydrogen bonding site from the aqueous media, similar to the concept of concave phenanthroline bases established by Lüning et al. [19].

The driving force for molecular recognition processes in water is generally the formation of hydrophobic interactions between (charged) hydrosoluble guests and the hydrophobic pocket of a water-soluble host. This concept was initiated in the early 80s by pioneering work on cyclophanes by Diederich, who aimed to mimic nature's strategy of burying a polar site within a hydrophobic pocket of a protein [20]. The concept was later extended to sophisticated cyclophanes such as calixarenes [21], resorcinarenes [22], pillarenes [23] or imprinted micelles [24], among others. The striking feature of **3Zn**-(TMe-β-CD)$_2$ as a receptor is that the binding enhancement can be clearly assigned to the protection of the hydrogen bonding site. If the CD contributed in another way to the enhanced binding, this effect would have also been detected for ZnTPPS-(TMe-β-CD)$_2$; however, this was not the case. Only the effects of steric encumbrance were observed, with no increased affinity for ImH compared to ZnTPPS alone.

This surprising hydrogen bond-directed recognition in an aqueous buffer for our host–guest complex suggests that discrimination of the distal vs. promixal site, previously observed in organic solvents, can be reproduced in aqueous media. The self-assembly of strapped porphyrins with cyclodextrins may lead to new concepts in the design of hemoprotein models and

investigation of the reactivity of paramagnetic ferric and ferrous complexes is currently under way.

EXPERIMENTAL

General methods

^{1}H NMR spectra were recorded on a JNM-ECA500 spectrometer (500 MHz) or a Bruker 500 spectrometer. Matrix-assisted laser desorption/ionization time-of-flight (MALDI-TOF) mass spectra were taken on a Bruker Daltonics autoflex speed spectrometer using an α-CHCA matrix or a dianthrol matrix (for **4Zn** only). Chemical shifts are given relative to the peak of the residual solvent: DMSO at 2.50 ppm, CHCl$_3$ at 7.24 ppm. UV-vis spectra were recorded on a Shimadzu MultiSpec-1500 photodiode-array spectrometer with a thermostatic cell holder or a Cary 5000 spectrometer. The starting material, porphyrin **1**, was synthesized according to a literature method [15]. Heptakis(2,3,6-tri-*O*-methyl)-β-cyclodetrin (TMe-β-CD) was purchased from Nacalai.

Determination of stability constants

Stability constants were determined according to a literature method [17]. Briefly, to aqueous phosphate buffer solution (pH 7) containing porphyrin species in a 1 cm cuvette were added aliquots of the stock solutions of TMe-β-CD, imidazole (ImH), or *N*-methylimidazole (*N*-MeIm). After each addition, the cuvette was gently mixed, placed in a thermostatic cell holder (25 °C) for 5 min, and the UV-vis absorption spectrum was measured. The titration curves obtained from the absorbance changes as a function of the additives were analyzed by a nonlinear least-squares method using a computer program (SPANA) [17]. The reproducibility of the data was checked by repeating all experiments at least three times.

Synthesis

Synthesis of 2. To a degassed solution of **1** (117 mg, 0.123 mmol) in toluene (15 mL) and methanol (3 mL) were added Pd(PPh$_3$)$_4$ (4 mg, 0.15 mmol), 1 mL of degassed 2 M Na$_2$CO$_3$ aqueous solution, and phenylboronic acid (33 mg, 0.27 mmol). The mixture was heated at 80 °C for 12 h. After cooling the mixture to room temperature, the organic layer was diluted in toluene and the solution was washed three times with a 30% NH$_4$OH aqueous solution. The organic phase was dried over Na$_2$SO$_4$, filtered and evaporated to dryness. The resulting solid was purified by silica gel column chromatography (CH$_2$Cl$_2$) to afford **2** (57 mg, 0.060 mmol, 49%). ^{1}H NMR (CDCl$_3$): ppm 8.75 (br s, 8H), 8.67 (d, *J* = 7.5 Hz, 2H), 8.56 (br s, 4H), 8.00 (d, *J* = 8.0 Hz, 4H), 7.92 (t, *J* = 7.5 Hz, 2H), 7.88

(d, *J* = 7.5 Hz, 2H), 7.82 (t, *J* = 7.5 Hz, 2H), 7.72–7.70 (m, 4H), 7.62 (br s, 2H), 7.56 (d, *J* = 8.0 Hz, 2H), 7.54 (s, 2H), 6.82 (d, *J* = 8.5 Hz, 4H), 6.58 (d, *J* = 8.5 Hz, 4H), -2.42 (br s, 2H). MS: *m/z* 943.1 (calcd. for C$_{68}$H$_{42}$N$_6$ [M + H]$^+$ 942.4).

Synthesis of 3. A solution of **2** (57 mg, 0.06 mmol) in concentrated H$_2$SO$_4$ (>95%) (30 mL) was heated at 70 °C for 48 h. After cooling to room temperature, the solution was further stirred for 72 h and then poured into the cold water (*ca.* 200 mL). The precipitated porphyrin was collected by centrifugation. The solid was washed several times with cold water. The solid was dissolved in 25% NH$_4$OH aqueous solution, and the solvent was then evaporated *in vacuo* to give **3** as a tetra-ammonium salt (52 mg, 0.04 mmol, 65%). ^{1}H NMR (DMSO-*d$_6$*): ppm 8.81 (d, *J* = 4.5 Hz, 4H) 8.78 (br s, 2H), 8.75 (d, *J* = 4.5 Hz, 4H), 8.61 (d, *J* = 8.5 Hz, 2H), 8.28 (d, *J* = 8.0 Hz, 2H), 8.22 (d, *J* = 7.5 Hz, 2H), 8.01 (d, *J* = 8.5 Hz, 2H), 7.91 (d, *J* = 8.5 Hz, 2H), 7.88 (d, *J* = 7.5 Hz, 2H), 7.82 (d, *J* = 8.5 Hz, 2H), 7.74 (s, 2H), 7.71 (d, *J* = 8.0 Hz, 2H), 6.81 (d, *J* = 8.5 Hz, 4H), 6.72 (d, *J* = 8.5 Hz, 4H), -2.67 (br s, 2H). MS (positive mode): *m/z* 1264.0 (calcd. for C$_{68}$H$_{43}$N$_6$O$_{12}$S$_4$ [M − 4NH$_4$ + 5H]$^+$ 1263.2). EA calcd. for C$_{68}$H$_{38}$N$_6$O$_{12}$S$_4^{4-}$·4NH$_4^+$·9H$_2$O: C, 54.68; H, 4.86, N, 8.38; found: C, 54.78, H, 4.49, N 8.16.

Synthesis of 3Zn. A mixture of **3** (8.2 mg, 6.5 μmol) and ZnO (17 mg, 0.21 mmol) in H$_2$O (25 mL) was refluxed for 2 days. After confirming the complete metalation by fluorescence spectroscopy, the mixture was cooled to room temperature. The excess ZnO was filtered off and the filtrate was concentrated to 1 mL *in vacuo*. The solution was passed through a Sephadex G-25 column to afford **3Zn** (2.2 mg, 1.7 μmol, 26%). UV-vis (phosphate buffer at pH 7.0) λ$_{max}$, nm (ε in M^{-1}·cm^{-1}); 430 (4.5 × 10^5), 561 (3.7 × 10^4), 605 (2.0 × 10^4). MS (negative mode): *m/z* 1324.0 (calcd for C$_{68}$H$_{39}$N$_6$O$_{12}$S$_4$Zn [M − 4NH$_4$ + 3H]$^-$ 1323.1).

Synthesis of 4Zn. A mixture of **3** (25 mg, 23 μmol) and zinc acetate (80 mg, 0.36 mmol) was refluxed in THF (10 mL), MeOH (5 mL) and pyridine (0.1 mL) for 2 days. The solution was cooled to room temperature and solvents were removed under vacuum. The residue was taken in water and sonicated. The slurry was filtered on a fritted glass funnel and the solid was washed with water. The solid was covered with MeOH (5 mL) and aqueous ammonia (5 mL). This slurry was sonicated for 5 min. The solvents were then removed under vacuum to afford **4Zn** as a black solid (17 mg, 14 μmol, 62%). ^{1}H NMR (500 MHz, DMSO-*d$_6$*): ppm 8.74 (d, *J* = 4.5 Hz, 2H), 8.67 (d, *J* = 4.5 Hz, 2H), 8.60–8.52 (m, 2H), 8.25 (d, *J* = 8.5 Hz, 2H), 8.01–7.91 (m, 4H), 7.91–7.84 (m, 4H), 7.79 (t, *J* = 7.5 Hz, 2H), 7.72 (s, 2H), 7.71 (d, *J* = 8.5 Hz, 2H), 6.76 (d, *J* = 8.5 Hz, 4H), 6.66 (d, *J* = 8.5 Hz, 4H). UV-vis (MeOH) λ$_{max}$, nm (rel. abs.): 286 (0.14), 312 (0.14), 407 (0.09), 430 (1), 562 (0.04), 602 (0.01). MS: *m/z* 1165.26 (calcd for C$_{68}$H$_{41}$N$_6$O$_6$S$_2$Zn [M − 2NH$_4$ + 3H]$^+$ 1165.18).

Acknowledgments

Supporting information

Additional spectral data for **3**, **3Zn** and Zn^{II}TPPS/TMe-β-CD, Figs S1–S9, are given in the supplementary material. This material is available free of charge *via* the Internet at http://www.worldscinet.com/jpp/jpp.shtml.

REFERENCES

1. Collman JP and Fu L. *Acc. Chem. Res*. 1999; **32**: 455–453.
2. Collman JP, Herrmann, PC, Boitrel B, Zhang X, Eberspacher TA, Fu L, Wang J, Rousseau DL and Williams ER. *J. Am. Chem. Soc.* 1994; **116**: 9783–9784.
3. Oohora K, Tang N, Morita Y and Hayashi T. *J. Biol. Inorg. Chem.* 2017; **22**: 695–703.
4. Ricoux R, Boucher JL, Mandon D, Frapart YM, Henry Y, Mansuy D and Mahy JP. *Eur. J. Biochem*. 2003; **270**: 47–55.
5. Mahy JP, Maréchal JP and Ricoux JD. *Chem. Commun.* 2015; **51**: 2476–2494.
6. Mosseri S, Mialocq JC, Perly B and Hambright P. *J. Phys. Chem* 1991; **95**: 4659–4663.
7. Kano K, Kitagishi H, Tamura S and Yamada A. *J. Am. Chem. Soc.* 2004; **126**: 15202–15210.
8. Kano K, Kitagishi H, Kodera M and Hirota S. *Angew. Chem., Int. Ed*. 2005; **44**: 435–438.
9. (a) Zhou H and Groves JT. *Biophys. Chem*. 2003; **105**: 639–648; (b) Zhou H and Groves JT. *J. Porphyrins Phthalocyanines* 2004; **8**: 125–140.
10. (a) Kano K, Kitagishi H, Dagallier C, Kodera M, Matsuo T, Hayashi T, Hisaeda Y and Hirota S. *Inorg. Chem*. 2006; **45**: 4448–4460; (b) Kano K, Ochi, T, Okunaka S, Ota Y, Karasugi K, Ueda T and Kitagishi H. *Chem. Asian J.* 2011; **6**: 2946–2955; (c) Watanabe K, Kitagishi H and Kano K. *Angew. Chem., Int. Ed*. 2013; **52**: 6894–6897.
11. Kitagishi H, Minegishi S, Yumura A, Negi S, Taketani S, Amagase Y, Mizukawa Y, Urushidani T, Sugiura Y and Kano K. *J. Am. Chem. Soc.* 2016; **138**: 5417–5425.
12. Lo M, Mahajan D, Wytko JA, Boudon C and Weiss J. *Org. Lett.* 2009; **11**: 2487–2890.
13. (a) Melin F, Trivella A, Lo M, Ruzié C, Hijazi I, Oueslati N, Wytko JA, Boitrel B, Boudon C, Hellwig P and Weiss J. *J. Inorg. Biochem.* 2012; **108**: 196–202; (b) Kahlfuss C, Wytko JA and Weiss J. *ChemPlusChem* 2017; **4**: 584–594.
14. (a) Brandel J, Trabolsi A, Melin F, Elhabiri M, Weiss J and Albrecht-Gary AM. *Inorg. Chem.* 2007; **46**: 9534.
15. Paul D, Melin F, Hirtz C, Wytko J, Ochsenbein P, Bonin M, Schenk K, Maltese P and Weiss J. *Inorg. Chem.* 2003; **42**: 3779–3787.
16. Vorburger P, Lo M, Choua S, Bernard M, Melin F, Oueslati N, Boudon C, Elhabiri M, Wytko JA, Hellwig P and Weiss J. *Inorg. Chim. Act.* 2017; **468**: 232–238.
17. Kano K, Nishiyabu R, Asada T and Kuroda Y. *J. Am. Chem. Soc.* 2002; **12**: 9937–9944.
18. (a) Adrian JC Jr and Wilcox CS. *J. Am. Chem. Soc.* 1991; **113**: 678–680; (b) Fersht A. *Trends Biochem. Sci.* 1987; **12**: 301–304.
19. Luning U, Baumstark R, Wangnick C, Muller M, Schyja W, Gerst M and Gelbert M. *Pure Appl. Chem*. 1993; **65**: 527–532.
20. (a) Diederich F and Dick K. *Tetrahedron Lett*. 1982; **23**: 3167–3170; (b) Diederich F and Dick K. *J. Am. Chem. Soc*. 1984; **106**: 8024–8036.
21. For recent examples: (a) Collin S, Parrot A, Marcelis L, Brunetti E, Jabin I, Bruylants G, Bartik K and Reinaud O. *Chem. — Eur. J.* 2018; **24**: 17964–17974; (b) Lascaux A, De Leener G, Fusaro L, Topić F, Rissanen K, Luhmer M and Jabin I. *Org. Biomol. Chem.* 2016; **14**: 738–746; (c) Peñuelas-Haro G and Ballester P. *Chem. Sci.* 2019; **10**: 2413–2423.
22. Haino T, Rudkevich DM, Shivanyuk A, Rissanen K and Rebek J Jr. *Chem. — Eur. J.* 2000; **6**: 3797–3805.
23. Shu X, Xu K, Hou D and Li C. *Isr. J. Chem.* 2017; **58**: 1230–1240.
24. Gunasekara RW and Zhao Y. *Org. Lett.* 2018; **19**: 4159–4162.